CrossMark

ORIGINAL PAPER

Monitoring the recent trend of aeolian desertification using Landsat TM and Landsat 8 imagery on the north-east Qinghai–Tibet Plateau in the Qinghai Lake basin

Haibo Wang[1,2] · Mingguo Ma[3] · Liying Geng[1,2]

Abstract As an important part of Qinghai Plateau, the Qinghai Lake is a sensitive and fragile zone for global change impacts. It is one of the most strongly desertified regions on the Qinghai Plateau. Based on remote sensing, a geographic information system and using Thematic Mapper imagery for the years 1987, 2000, 2009 and Landsat 8 images for the year 2014 as data sources, we extracted information regarding the dynamic changes of aeolian desertification in the study area over the last 28 years. The spatio-temporal evolutions of the landscape patterns of regional aeolian desertified land (ADL) are discussed. Our objective is to provide references for desertification control and eco-environmental restoration in the Qinghai Lake basin (QLB). Results elicit an aeolian desertified area which has increased by 96.74 km^2 over the past 28 years. ADL mainly experienced processes of increasing stable to decreasing trends, before 2000, the area of aeolian desertification increased by 338.03 km^2. After 2000, desertification remains stable, but as we speak desertification decreases and a moderate and slight ADL took the lead. The dynamics of aeolian desertification in QLB is mainly determined by climate change, human activities and management.

✉ Haibo Wang
    wanghaibokm@163.com

1   Heihe Remote Sensing Experimental Research Station, Cold and Arid Regions Environmental and
    Engineering Research Institute (CAREERI), Chinese Academy of Sciences, 320# Donggang West
    Road, Lanzhou 730000, Gansu, China

2   Key Laboratory of Remote Sensing of Gansu Province, Cold and Arid Regions Environmental and
    Engineering Research Institute (CAREERI), Chinese Academy of Sciences, Lanzhou 730000,
    China

3   School of Geographical Sciences, Southwest University, Beibei, Chongqing 400715, China

🍃 Springer

1 Introduction

Dryland covers 40 % of the Earth's land surfaces and offers shelter to 20 % of the worldwide population (Roberto 2002). Aeolian desertification is one of the most devastating environmental and socio-economic problems in arid, semi-arid and dry semi-humid climate zones (Wang et al. 2012). Aeolian desertification destroys land resources, reduces ecosystem productivity, depresses ecosystem services and exacerbates poverty (Duan et al. 2014). Nonetheless, aeolian desertification occurring on the high-altitude areas of the Qinghai–Tibet Plateau (QTP) only recently attracted attention (Shen et al. 2012; Hu et al. 2015). The majority of the QTP is located at altitudes higher than 3000 m. Hence, climate in the QTP is cold. Mean annual temperature for the entire plateau area has, however, increased significantly since the 1960s (You et al. 2010).

The Qinghai Lake is the largest plateau, inland salt-water lake of China, located in the north-eastern region of the QTP. The Qinghai Lake basin (QLB) is an important part of QTP and is very sensitive and vulnerable to global change impacts. During the last decades, since the change of natural environment conditions (i.e. climate warming), and the increasing impacts of anthropogenic activities (over grazing and excessive farming), a series of severe eco-environmental problems has occurred. They include the decline of the lake water levels, pasture retrogression, vegetation sparsity, wetland shrinkage and land desertification (Yu and Chen 2002) exacerbated in the circumference of the Qinghai Lake zone. Land desertification became one of the most heaviest ecological environmental problems in the QLB. Increasing desertification became an important factor restricting the exploration of resources as well as the sustainable economic and social development. Consequently, studying land desertification in QLB and describing the dynamics of land desertification status, characteristics, and evolution patterns and trends accurately and in time are of prime importance. Analysing the driving factors of the desertification is of great scientific importance for watershed resource development and especially its environmental protection. The important eco-environmental role of this region highlights the urgency to study the evolution of aeolian desertification to better understand its driving forces.

Over the past few years, land desertification in the lake zone range of the Qinghai Lake expanded rapidly, exhibiting a ring-belt spread around the lake. The lake has always been a hot spot on the QLB (Zhang et al. 2011; Guo et al. 2010; Hu et al. 2012; Zhan and Yan 2012; Zhao et al. 2015) for researchers. During recent years, a large number of scholars conducted comprehensive analysis of the dynamics, causes, degradation and countermeasures for land desertification in research, which is mainly based on RS and geographic information system (GIS) applications. Interpretation of remote sensing (RS) imagery has been performed to analyse the dynamics of land desertification differences in classification systems of land cover and approaches of land desertification in QLB, and the monitoring approach of land desertification in QLB is different. For example, Hu et al. (2012) state that the land desertification of QLB has increased rapidly during the period from 1995 to 2006. This research predicted that the area of the land desertification will consistently increase during the first 15 years of the next two decades. Zhao et al. (2015) thought desertification is relatively stable and has slightly shrinked during the twentieth century. To summarize, the present situation of researches is limited. Most of results are based on the RS imagery from before 2010, lacking the latest findings on the monitoring on desertification during recent years. Because of the importance of eco-environmental and socio-economic activities in this region, since 2008, the Chinese government has invested more than one billion RMB to manage the environmental problems in this region, including

aeolian desertification. However, it is necessary to reassess the present situation of land desertification in QLB and obtain information on whether the eco-environmental and land desertification of the QLB has improved or not.

Multi-temporal RS data provide an opportunity to extract spatio-temporal information on aeolian desertification (Gao and Liu 2010; Yan et al. 2009). In particular, multi-spectral satellite sensors, such as Landsat MSS, TM and ETM+, are important tools for land desertification monitoring, at the regional scale (Liberti et al. 2009; Alatorre and Beguería 2009). At the same time, since the strip noises of the Landsat 7 satellite and the retirement of Landsat 5 satellite in recent years, for the purpose of extending the Landsat record into the future and maintaining continuity of observations, the satellite Landsat 8 alternatives have successfully been launched in 2013 which is very important for global change research (Roy et al. 2014). However, since launch time was not long, research on the extraction of desertification information based on Landsat 8 satellite images turns out to be relatively rare at present.

Hence, this paper aims to monitor the spatio-temporal patterns and dynamics of aeolian desertification by means of Landsat TM and Landsat 8 data from four dates (1987, 2000, 2009 and 2014) in the QLB. This allowed to elucidate the driving forces of aeolian desertification and its sensitivity to climate change and human activities. The results provide useful information fostering the comprehension of complex desertification processes and its dynamics. It will help to control and manage desertification in this region.

2 Study area

The QLB is located in the north-eastern part of the QTP in the Qinghai province of China (Fig. 1). It lies between latitudes 36°15′ and 38°20′N and longitudes 97°50′ and 101°20′E, with altitudes between 3194 and 5129 m, covering an area of 29,664 km². The Qinghai Lake located in the QLB, north-eastern of Qinghai province, has a water surface area of 4282 km² and an altitude of 3196 metres. It is one of the highest lakes in China. The circumference of the Qinghai Lake zone includes three counties in the Qinghai province (Gonghe County of the Hainan Tibetan autonomous prefecture, Gangcha County of Haibei Tibetan autonomous prefecture and the Hercynian Mongolian Tibetan autonomous prefecture of Tianjun County). Including the Qinghai Lake, the area of this region is 15,979 km², consisting of 54 % of the total of QLB. Figure 2 shows the location of QLB. The vegetation in this region is dominated by alpine meadow. There is a stretch of shore dunes at the lakeside, especially at the eastern coast of the Qinghai Lake.

During recent years, land desertification became dominant problem area, which affected local economic and social development. The QLB has a semi-arid, frigid and monsoon climate due to its high altitude. It is characterized by a dry, windy climate with intense solar radiation and a large seasonal temperature span. Mean annual precipitation ranges from 191 to 515 mm. Mean annual evaporation ranges from 1300 to 2000 mm (Zhao et al. 2015), and mean annual temperature ranges from −3.4 to −1.7 °C. The circumferencing lake zone of the QLB is a convergence zone of the eastern and QTP monsoons. They prevail perennially by north-west winds with more than 150 days of sand carrying wind speeds with annual mean wind speeds larger than 5 m/s (Hu et al. 2012). The region of the Qinghai Lake is an important production region of animal husbandry in the Qinghai province. Its cropping industry, tourism and industrial production capacity reached a higher
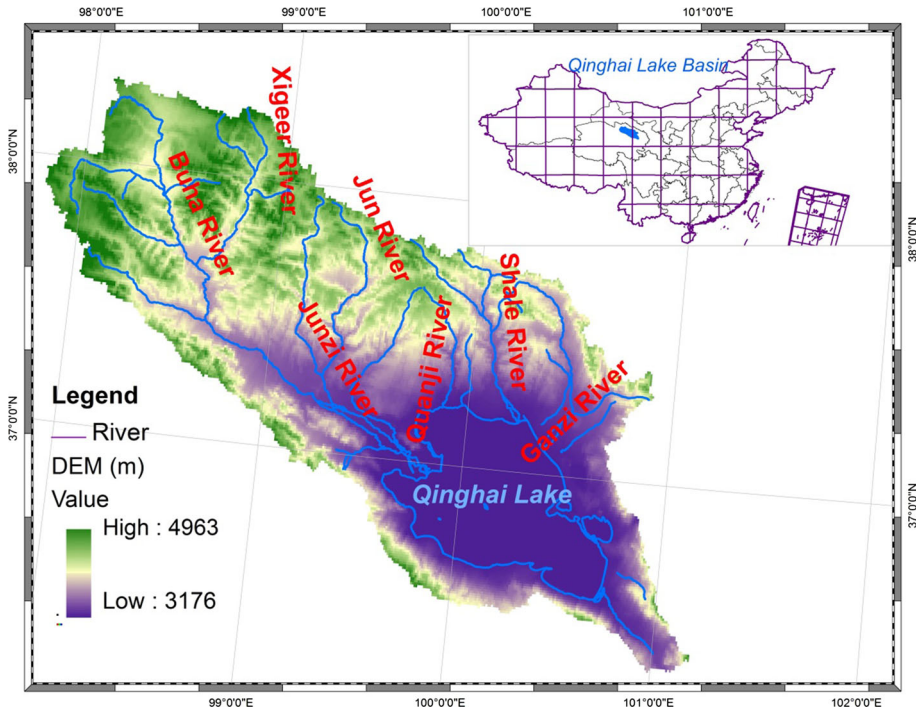
Fig. 1 Location of the Qinghai Lake basin

scale of development, and it is one of the regions in the Qinghai province with relatively intensive human activities.

3 Materials and methods

3.1 Data sources

To achieve the research objective of the dynamic monitoring of aeolian desertification taking place in the region around the Qinghai Lake, Landsat Thematic Mapper (TM) imagery acquired in 1987, 2000 and 2009 as well as Landsat 8 images obtained in 2014 as the data source was used. RS imagery of cloudless days or days with a cloud cover of no more than 10 % in the vegetation growing season has been selected. They mainly originate from the site (URL) http://glovis.usgs.gov/ (Table 1). The growing season of vegetation, normally from May to September, is considered as a favourable time to extract and identify the information of land desertification with RS imagery. Vegetation has a vigorous growth in that period and a maximal coverage fraction during that period. Hence, land with or without aeolian desertification can easily distinguished with the RS imagery. Additionally, ancillary reference data with respect to the study region provided by "Cold and Arid Regions Science Data Center at Lanzhou" in CAREERI (URL, http://westdc.westgis.ac.cn), and the Data Center for Eco-Environment Protection in the QLB, include DEM data,
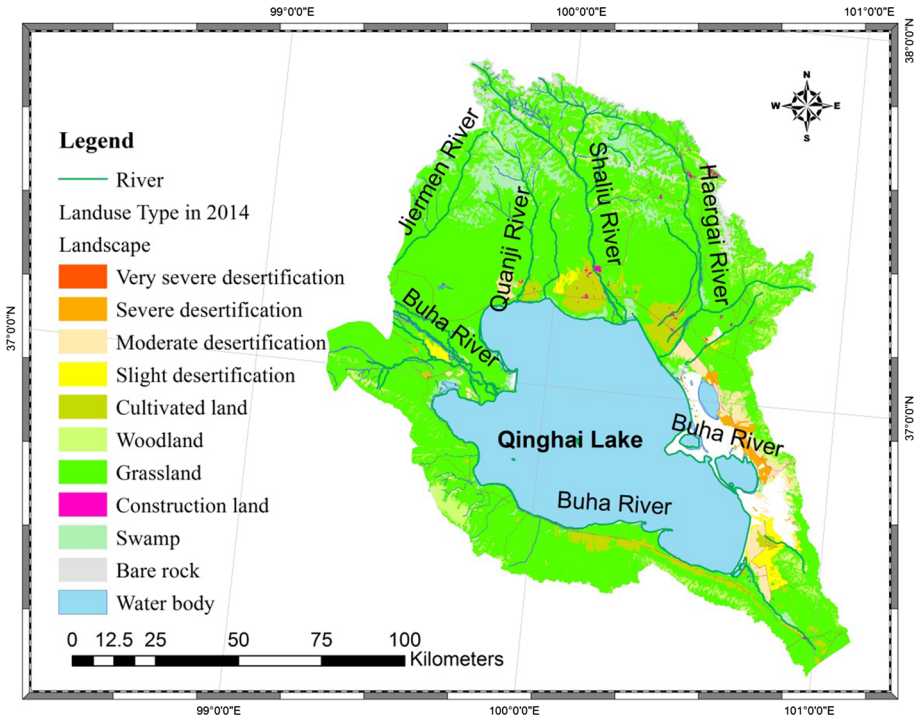
Fig. 2 Distribution of land use in the region around the Qinghai Lake watershed

river course data and land use and land cover data (Liu et al. 2003), selected as supplementary data sources.

Meteorological data, from the China Meteorological Data Sharing Service System, include precipitation, temperature and wind velocity data, recorded from 1958 to 2014 by local meteorological stations (37°20′, 100°08′, and at a height a.s.l. of 3301.5 m), Gangcha County, in the circumferencing zone of the Qinghai Lake. They were collected to analyse the impact of the dynamics of aeolian desertification around Qinghai Lake. It was investigated by the introduction of the water deficiency index how the driving forces of aeolian desertification are elicited. The aeolian desertification around QLB is quite strongly coupled with this region's water deficit which is a connecting factor between precipitation and evaporation and the difference between them. We calculated evaporation (E) of QLB based on an empirical equation of evaporation according to Eq. (1) (Ding and Liu 1995):

Table 1 Data applied in monitoring aeolian desertification around Qinghai Lake

Item	Image acquisition date (year-month-day)	Orbit number	Data source
1	1987-08-15	133/034, 133/035	Landsat TM
2	2000-08-18	133/034, 133/035	Landsat TM
3	2009-08-11	133/034, 133/035	Landsat TM
4	2014-06-25	133/034	Landsat 8
5	2014-05-07	133/035	Landsat 8

$$E = 1017.9 + 86.9 * T + 0.1 * V - 0.98 * P, \tag{1}$$

with T, temperature (°C); V, wind velocity (m/s); P, annual average precipitation (mm).

3.2 Image processing and interpretation

3.2.1 Classification system for aeolian desertified land

The establishment of a classification system for aeolian desertified land (ADL) was elaborated prior to the extraction of desertification information by RS. Discrepancies occur in classification systems for land desertification variable from one study to another. According to the intensity of aeolian sandy activities in each area, different scholars as mentioned earlier applied different classification system of desertification classification methods which can be roughly summarized into three methods:

1. the ADL around the lake is divided into four grades: potential, developing, intensively developing and severe when referring to the literature (Yu and Chen 2002; Zhang et al. 2011);
2. the ADL was classified as extremely severe desertification, severe desertification, moderate desertification, mild desertification and potential desertification (Zhao et al. 2015);
3. the intensity of desertification is divided into four categories: extremely severe, severe, moderate and slight according to Hu et al. (2012).
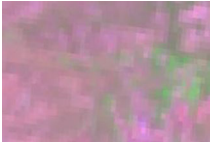
In the first method, potential ADL refers to natural conditions which are likely to transform into desertified land, but where the land has not been transformed into desert yet. This type of category covers a wide range but shows large discrepancies in its results (e.g. Yu and Chen 2002; Zhang et al. 2011). The classification system of the second category is more comprehensive. Knowledge of general varying characteristics of ADL, however, is to a certain degree influenced by the difficulty in interpreting potential desertification from RS imagery (Zhao et al. 2015). Therefore, a third-class classification system was developed which is currently more popular.

Under such circumstances, reference is made to the national standard technology procedures for monitoring desertified land, combined with the actual status of QLB, to divide land use into farmland, forests, built-up land, water bodies, desertified land, saline and alkaline land, marshland and fallow lands. Referring to the already existing standards for classifications of land desertification proposed in previous studies (e.g. Wang et al. 2012, 2013; Yan et al. 2009; Duan et al. 2014), we chose the proportions of the area covered by mobile sand dunes or wind-eroded lands, and vegetation coverage as the main indices used to reflect the severity of aeolian desertification status (Duan et al. 2014), and applied the third method which is popular in other arid and semi-arid regions in the north of China (Yan et al. 2009; Duan et al. 2014), to classify intensities of desertification as slight, moderate, severe and extremely severe. Table 2 elicits the details of the classification system, as well as samples of the results obtained by interpreting part of Landsat TM and Landsat 8 imagery using these criteria.

3.2.2 Information extraction of ADL using remote sensing

RS imagery is visually interpreted using RS and GIS software by exploiting land marks defined by typical training areas. The RS imagery has been processed with RS software to

Table 2 Classification system of aeolian desertification by remote sensing monitoring in Qinghai Lake watershed

Degree of aeolian desertification	Types of sandy desertified land	Landscape features	Landsat TM (5/4/3 wave band combinations)	Landsat 8 (6/5/4 wave band combinations)
Extremely severe	Mobile sand dune, wind-eroded inferior land	Serried shifting sand dune is overwhelming predominated; with sparse or almost no vegetation presence. Shifting land area >50 %, vegetation coverage <5 % (% of total land area)		
Severe	Semi-mobile sand, wind-eroded residual hill	Shifting sand has largely distributed, wind erosion intensively emerged. Shifting land area 25–50 %, vegetation coverage 5–20 % (% of total land area)		
Moderate	Semi-fixed sand dune, bare sandy gravel	Small piece of shifting sand emerged, combining with wind drift nebkhas and wind erosion. Shifting land area 5–25 %, vegetation coverage 20–50 % (% of total land area)		
Slight	Fixed sand dune, semi-bare sandy gravel land, construction control land	Shifting land has not yet largely appeared, but its spots can be accidentally witnessed. Shifting land area <5 %, vegetation coverage >50 % (% of total land area)		

perform band composition, image enhancement and geometric correction. By comparing the TM bands of LANDSAT imagery and their relation with the study region, we could draw lessons from these researches (Yu and Chen 2002; Jing et al. 2011). It was found that the wavelength bands 3, 4 and 5 of the TM sensor and 4, 5 and 6 of the Landsat 8 sensor combined included an abundant amount of information. As a result, the study adopted the spectral band TM 5, 4, 3 combinations, the Landsat 8 spectral band 6, 5, 4 compositions and a R/G/B resultant image in classification and interpretation to refine the representation of desertification information. Under the influence of these spectral band combinations, vegetation growth and ADL were highlighted obviously and with better visual effects, which was advantageous to the information extraction of ADL.

RS software has been applied for geometric corrections of the imagery; its precision for plain areas is less than one pixel and no more than two pixels for mountainous areas. Through field research, selecting in the field various and representative types of ADL, in combination with RS imagery and related literature, the correspondence between surface features of different degrees and types of desertification elicited by the RS imagery was established and interpreted (Fig. 2).

According to the established interpretation samples in Landsat TM and Landsat 8 imagery using the classification criteria and the geography comprehensive analysis method, we conducted the visual interpretations for extracting information of aeolian desertification by applying GIS software. In addition to the Landsat TM and Landsat 8 imagery, we used ancillary materials such as topographic maps, vegetation maps, land cover maps and field survey reports to assist in interpreting the types of desertification in each mapped area during the interpretation process. Meanwhile, we superimposed, compared, inspected and rectified our interpreted results with the support of high-resolution RS imagery obtained from Google Earth©. With the enhanced quality and accuracy of image interpretation, we obtained information regarding ADL or different yearly periods.

3.2.3 Dynamic monitoring methods of aeolian desertification

With the support of ArcGIS and ENVI, we applied the overlaying function module of GIS to perform an overlay analysis as well as spatial statistics for the monitoring of aeolian desertification for different phases. Methods were adopted for spatial–statistical analysis such as the transfer matrix of landscape types, to quantitatively analyse spatio-temporal changes of ADL in the study area. The transfer matrix of landscape types clearly reflected transformations of a variety of landscape types, which is of great value for the analysis of the dynamics and causes of landscape ecology. Landscape dynamic attitude is a reflection of the changes in amplitude and rates of variation rate for different land use types in unit time and cover type discrepancies in the change of regional land use. This is summarized in Eq. (2):

$$DC = (Ua - Ub)/Ub/T \times 100\%, \tag{2}$$

where DC is the dynamic rate of change (%) of landscapes in T years; Ub stands for areas of landscape in the initial stage of the study (km^2); Ua is the area of landscape in the terminal stage of the study (km^2); T is time (years).

4 Results and analysis

4.1 Analysis of the current status of ADL around Qinghai Lake

The current status of ADL around the Qinghai Lake (Fig. 2) has been acquired by means of a RS extraction method for desertified surfaces, a classification system and interpreted RS imagery of Landsat 8. The statistical data of the areas in the study region (Table 3) have been obtained by statistical analysis. According to survey results, the total area of ADL around Qinghai Lake is 1039.72 km^2, which accounts for 6.51 % of the total study area. Most of its are extremely severe ADL processes with an area of 469.78 km^2, occupying 2.94 % of the total study region. Second is moderate ADL with an area of 318.93 km^2, covering 2.0 % of total study area. An area of slight and serve ADL is, respectively, 161.80 and 89.21 km^2, occupying 1.01 and 0.56 % of the total study region, respectively. The areas of un-desertified lands were 14,939.40 km^2, mostly covered with grassland having an area of 8207.71 km^2. Water bodies occupy an area of 4583.70 km^2, taking 51.37 % of the study area.

Figure 2 shows the spatial distribution of ADL with varying degrees. The ADL is distributed in annuluses circumferencing the Qinghai Lake and mainly clustered together with linked pieces, forming a large sandy area at the East Lake, Ganzi River and Bird Island, etc. The extremely severe desertification area is mainly distributed in the koto sandy area, at the east coast of the lake and the north-east Sandy Island; severe desertification land surrounded the region of extremely severe desertification, centralized in downstream region of the Ganzi River, the north shore of Lake and eastern area of Koto. Moderate and slight desertification distribution is more fragmented.

Table 3 Statistics of aeolian desertification in the region around Qinghai Lake watershed

Landscape	Land use classification	Area/km^2	Percentage/%
Desertification land	Extremely severely desertified land	469.78	2.94
	Severely desertified land	89.21	0.56
	Moderately desertified land	318.93	2.00
	Slightly desertified land	161.80	1.01
Total	–	1039.72	6.51
Lands without desertification	Farmland	480.27	3.01
	Grassland	8207.71	51.37
	Forests	575.30	3.60
	Built-up land	81.71	0.51
	Water bodies	4583.70	28.69
	Marshland	724.97	4.54
	Bare rock gravel	285.74	1.79
Total	–	14,939.40	93.49

4.2 Distribution of desertification

4.2.1 Spatial and temporal dynamic changes of ADL

Based on the analysis of the dynamic evolution of ADL around Qinghai Lake during recent 28 years by analysing changing data ranging from four periods of land desertification in the circumference of the Qinghai Lake zone, it can be found that during 1987–2014, large changes have taken place in the area of ADL around Qinghai Lake. These changes have evolved from an initial period of rapid growth to a relatively stable period and then gradually to a period of decreasing change (Table 4; Fig. 3). The total area of ADL surrounding Qinghai Lake in 1987, 2000, 2009 and 2014 was 942.99, 1281.02, 1273.36 and 1039.72 km^2, respectively, accounting for 5.90, 8.02, 7.97 and 6.51 % of the total area, respectively. Generally, extremely severe ADL expansion took place from 1987 to 2014 with only a small increase during 1987–2000. The severe ADL phase showed an increasing trend before 2000 but then gradually decreased after 2000; the tendency of moderate ADL is basically in accordance with severe ADL phases, but shares a time lag for its decline. The area of slight ADL differences changed slightly before 2009, but increased rapidly during recent years, demonstrating the phenomenon that ADL is shrinking. Compared with 1987, total desertified surface area has known a marginal growth during the past 28 years, with an increased area of 96.74 km^2 and a dynamic degree of 0.37 % (Fig. 3).

The desertification in the region around Qinghai Lake expanded rapidly from 1987 to 2000. Different types of ADL expanded vigorously and their intensity exacerbated, eco-environment deteriorated in this region. The total surface area of ADL increased with 338.03 km^2 over the past 13 years, with a growth dynamic of 2.76 %. Moderate and severe ADL increased most of all, respectively, with an area of 153.61 and 113.48 km^2. Each type of dynamics degree amounted to was 4.38 and 4.32 %, respectively. The extremely severe ADL as well as slight ADL's grew into areas of 67.93 and 3.01 km^2, respectively, with dynamics amounting to degrees of 1.15 and 1.31 %.

In the time period from 2000 to 2009, ADL tended to stabilize with a slight trend of decrease. During nearly 9 years, the total area of ADL decreased mildly (with a reduction in 7.66 km^2) and with a dynamics degree amounting to -0.07 %. The areas with extremely severe desertification dropped sharply, respectively, to 163.77 and 53.99 km^2, respectively. The dynamic degrees amount to -5.76 and -1.15 %, respectively. The area of slight desertification decreased a marginally (with -13.94 km^2), basically a stabilization. Moderate ADL increased, however, with 224.04 km^2 with a dynamic degree of 5.88 %.

Desertification apparently decreased in the period from 2009 to 2014, the area of ADL tapered off little by little during almost 5 years, with a reduction in 233.63 km^2 and dynamic degree of -3.67 %. The areas of moderate and severe desertification decreased, respectively, with 328.53 and 62.76 km^2, respectively, each with a dynamic degree of -10.15 and -8.26 %, respectively. While area's with a slight desertification increased significantly, with a rate of 155.04 km^2 per year. It can be seen that the intensity of land desertification eased off over recent years. The ecological environment of QLB has thereby been significantly improved as well.

4.2.2 Landscape desertification transfer

A landscape transfer matrix can be used to characterize structures and features of change for regional land use and transfer vectors for each land use type. This is conducive to

Table 4 Dynamics of desertification landscape around the Qinghai Lake

| Degree of desertification	1987–2000			2000–2009			2009–2014		
	1987 Area/km²	Variable quantity/km²	Dynamic rate/%	2000 Area/km²	Variable quantity/km²	Dynamic rate/%	2009 Area/km²	Variable quantity/km²	Dynamic rate/%
Extremely severe	453.22	67.93	1.15	521.16	−53.99	−1.15	467.16	2.62	0.11
Severe	202.26	113.48	4.32	315.74	−163.77	−5.76	151.97	−62.76	−8.26
Moderate	269.81	153.61	4.38	423.42	224.04	5.88	647.46	−328.53	−10.15
Slight	17.70	3.01	1.31	20.70	−13.94	−7.48	6.77	155.04	458.33
Total	942.99	338.03	2.76	1281.02	−7.66	−0.07	1273.36	−233.63	−3.67
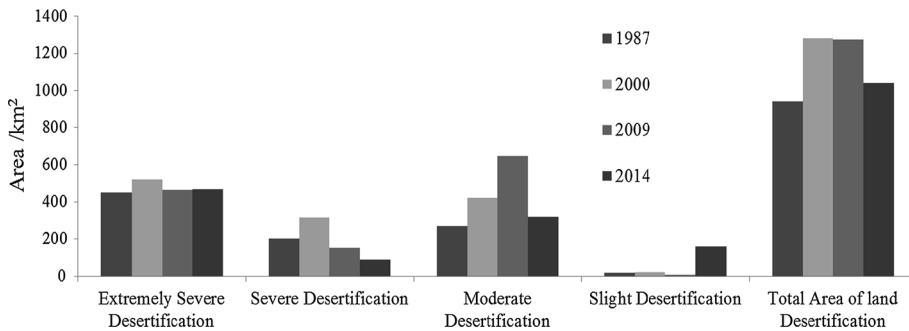
Fig. 3 Area changes of different types of desertification per indicated year

understand the whereabouts and losses of various types of land use. It also allows to better study the source and composition of each terminal type of land use. Using the spatial analysis function of GIS, a landscape transfer matrix over three periods of ADL (1987–2000, 2000–2009 and 2009–2014) as well as other types of land use at Qinghai Lake was acquired (Table 5).

Between 1987 and 2000, different levels of ADL increased and desertification tended to expand. Land use types with extreme desertification converted slightly to other types of ADL, 20.16 km^2 of severe ADL redirected into extremely severe ADL. The other 26.0 km^2 decreased to a moderate ADL. There are 110.55 km^2 of moderate ADL which transformed into severe ADL. Land use areas with slight desertification transformed less than those of ADL evolved from other land use types. There are 324.03 km^2 of these lands transformed into moderate desertification.

Desertification remained relatively stable during the period from 2000 to 2009. It nevertheless tended to slightly shrink in surface area. Indications were gathered that some very severe and severe ADL tended to moderate ADL, with a reversion area of 48.32 and 150.18 km^2, respectively. Concomitantly, a deterioration tendency of desertification emanated in some areas. An example of such an area (22.54 km^2) was severe ADL transformed into extremely severe ADL proved the trend. Conversion from moderate ADL and the other types of lands occurred frequently. Land areas with moderate desertification evolved from 12.21 to 25.78 km^2, respectively, to extremely severe and severe desertification.

There are severe ADL's shrinking to moderate ADL as well. Part of moderate ADL's to slight ADL occurred with a reversion area of 113.61 and 117.35 km^2, respectively.

4.2.3 The evolution of desertification spatial patterns surrounding Qinghai Lake

Spatial patterns of land desertification in the region around Qinghai Lake changed strongly over the period from 1987 to 2014. The evolution of desertified landscape patterns around Qinghai Lake for different periods (Fig. 4) was mapped by using the spatial analysis tool of ArcGIS software. From 1987 to 2000, land desertification elicited an increasing trend.

It has been found that an increased number of extremely severe ADL types have partially derived from non-desert land. Primarily, these have been shaped by emerging sediment due to the reduction in water bodies. Remaining parts were formed by degradation to severe desertification. Severe ADL was a transformation of extremely severe

Table 5 Transfer matrix in different types of aeolian desertification around the Qinghai Lake during recent 28 years

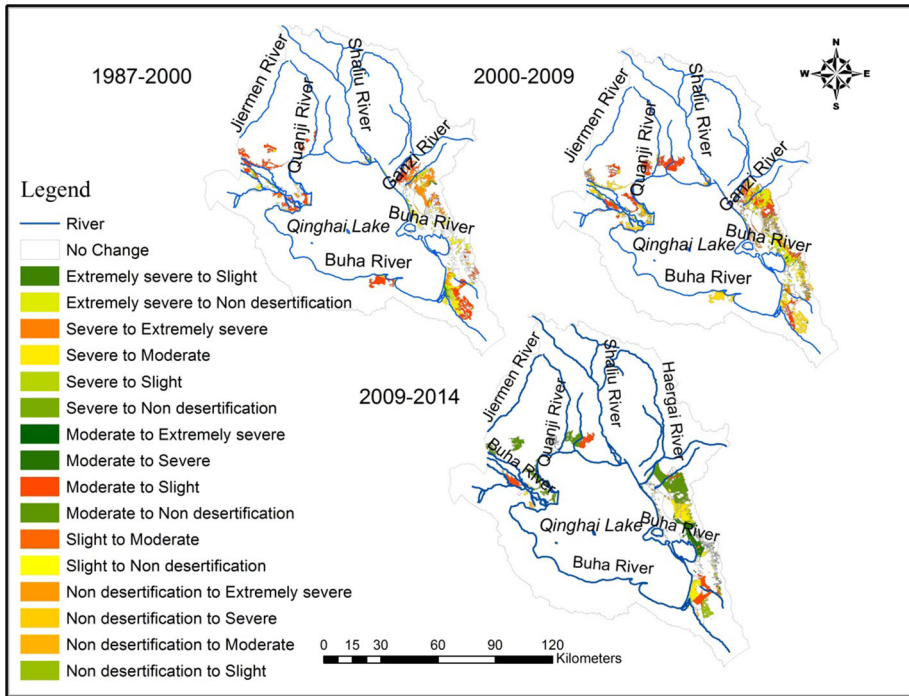| Periods	Types of desertification	Very severe desertification/km²	Severe desertification/km²	Medium desertification/km²	Slight desertification/km²	Other land/km²
1987–2000	Very severe	448.92	2.43	0.69	0.11	1.05
	Severe	20.16	147.16	26.00		8.68
	Medium	5.42	110.55	70.56	1.71	81.35
	Slight		0.46	2.40	5.13	9.72
	Other	46.65	55.08	324.03	13.75	14,595.45
2000–2009	Very severe	393.84	11.21	48.32	1.58	66.20
	Severe	22.54	84.99	150.18	0.34	57.63
	Medium	12.21	25.78	143.58	0.52	241.33
	Slight	0.90	1.20	3.98	0.95	13.68
	Other	37.67	28.65	301.38	3.38	14,325.51
2009–2014	Very severe	462.24			0.55	4.37
	Severe	3.44	18.89	113.61	6.13	9.90
	Medium	1.23	68.70	183.88	117.35	276.29
	Slight			0.30	4.60	1.87
	Other	2.87	1.61	21.13	33.18	14,646.98

Fig. 4 Dynamics of the spatial patterns of aeolian desertification around Qinghai Lake during the most recent 28 years

desertification and was distributed principally in the downstream sandy areas of the Ganzi River basin. Moderate ADL spreading around the Buha River basin has been created principally because of grassland degradation, second to the degradation in severe desertification. Slight ADL occurred mostly due to grassland degradation.

Land desertification stabilized mostly in the period from 2000 to 2009. Most of this process took place in the eastern parts of the Lake, e.g. in the sandy areas of Ketu and downstream the Ganzi River basin. Part of the very severe and severe ADL nevertheless transformed into moderate ADL. This reflected the management of the desertifying watershed had gradually been taken seriously in this period. As a result, some desertificating regions have been taken under more control. From 2009 to 2014, land desertification was declined. The areas and intensities of desertification were controlled more and step by step. The changes of areas with artificially fixed sand dunes in the eastern lake Ketu sandy region increased, and sandy grasslands in some areas thrived well. A general trend of a shrinking desertification was elicited with degrees from severe to moderate and finally to slight. It can be observed that prevention and desertification management around QLB did achieve a certain degree of success. As a result, the quality of the ecologically systems in this area has improved.

5 Discussion

5.1 Comparison with related studies

Current results on the dynamic monitoring of desertification in the QLB are summarized in Table 6. Certain discrepancies for the monitoring by different scholars are elicited by comparison. This may be caused by a different desertification classification systems applied by the scholars as well as an imparity for each monitoring year. As summarized in the section of Methodology, the classification systems of aeolian desertification level used in other arid and semi-arid regions in the north of China are often three- or four-level hierarchical classification system (Yan et al. 2009), different scholars as mentioned earlier applied different classification system of desertification classification methods (Table 6), which influenced the interpreted results of aeolian desertification. Referring the existed studies (e.g. Yan et al. 2009; Wang et al. 2012, 2013), we applied the "four-division" method domestically popular as well as overseas (Duan et al. 2014).

Compared to other studies of the type in this paper, the monitoring area of ADL around Qinghai Lake is comparatively close to that defined by Hu et al. (2012). This paper, however, illustrates a different trend of dynamic evolution for desertification. There are certain differences in RS imagery from 1 year to another, hence with an impact on the results of each year compared. Hu et al. (2012) exploited two periods of RS data ranging from 1995 to 2006 and suggested that desertification undergoes a process of expansion from slow rates to fast ones. However, the deviation from the prediction of dynamic trends

Table 6 Comparison between this study and other related findings

Ages	Years	Classification system	Total area of desertification (km^2)	Dynamic trends of the desertification development	References
1980s	1986	Method (1)	756.6	Developing	Yu and Chen (2002)
	1987	Method (1)	5756.91[a]	Developing	Zhang et al. (2011)
	1987	Method (3)	962.59	Developing	Hu et al. (2012)
	1987	Method (2)	1005.54	Developing	Zhao et al. (2015)
	1987	Method (3)	942.99	Developing	This study
1990s	1995	Method (3)	1044.07	Developing	Hu et al. (2012)
	2000	Method (1)	1247.80	Developing	Yu and Chen (2002)
	2000	Method (2)	1054.76	Relatively stable	Zhao et al. (2015)
	2000	Method (3)	1281.02	Relatively stable	This study
2000s	2004	Method (2)	1046.81	Slightly shrinking	Zhao et al. (2015)
	2006	Method (1)	5807.03[a]	Developing	Zhang et al. (2011)
	2006	Method (3)	1358.02	Developing	Hu et al. (2012)
	2009	Method (3)	1273.36	Relatively stable	This study
2010s	2010	Method (2)	1031.88	Slightly shrinking	Zhao et al. (2015)
	2011	Method (3)	1476.27[b]	Developing	Hu et al. (2012)
	2016	Method (3)	1604.82[b]	Developing	Hu et al. (2012)
	2014	Method (3)	1039.72	Shrinking	This study

[a] The result including the area of potentially desertified land

[b] Means the forecast result

for desertification is the result of the lack of introducing RS data during 2000 and after 2006. Results regarding the trend of dynamic evolution for desertification in this paper are similar to those of Zhao et al. (2015). Both considered that desertification tends to be relatively stable and then decreases from 2000 onwards.

5.2 Analysis of the causal origins of desertification in the QLB

Dynamic changes of desertification in QLB are affected by a combined impact of natural and anthropogenic factors. The development of desertification is controlled by climate change to a large extent (Wang and Ha 2004). Among the climate factors, precipitation and temperature are the more important contributors to desertification (Wang et al. 2005). It has been documented that desertification elicited a hysteresis relative to climate change (Duan et al. 2014), so meteorological data in Gangcha County covering the period from 1958 to 2014 in the regions around Qinghai Lake (Figs. 5, 6) have been selected. Furthermore, the relevant variables over a 5-year moving average have been calculated to analyse the drivers of desertification.

According to Fig. 5, the annual mean growth rate was 0.028 °C/year, which is higher than China's mean warming rate in the past 40 years (0.004 °C/year) and that of the global average warming rate in the past century (0.005 °C/year; Shi et al. 2003). Under arid conditions, higher temperatures will increase evapotranspiration, which increases the evaporative demand (Wang et al. 2013). According to the study of Le Houérou (1996), every 1 °C temperature increase can increase potential evapotranspiration by approximately 75 mm/year. Thus, during our study period, the increased temperature corresponds to a potential increase of about 2.1 mm/year of annual evapotranspiration. Nevertheless, precipitation increased slightly during the same period, by about 0.809 mm/year (Fig. 6). The increase in precipitation is lower than that of evaporative demand, evaporation volumes in the QLB are far more intense than precipitation volumes, and therefore, climate conditions in the QLB become increasingly arid during the study period.

In general, according to the basin meteorological data (Fig. 5, 6), QLB climate generally tends to warm up and to become dryer during recent years. Therefore, these simultaneous changes in temperature and precipitation likely increased the rate of aeolian desertification by creating more stress on the vegetation dynamics. The ecological environment in the area was intrinsically very fragile and was prone to desertification.
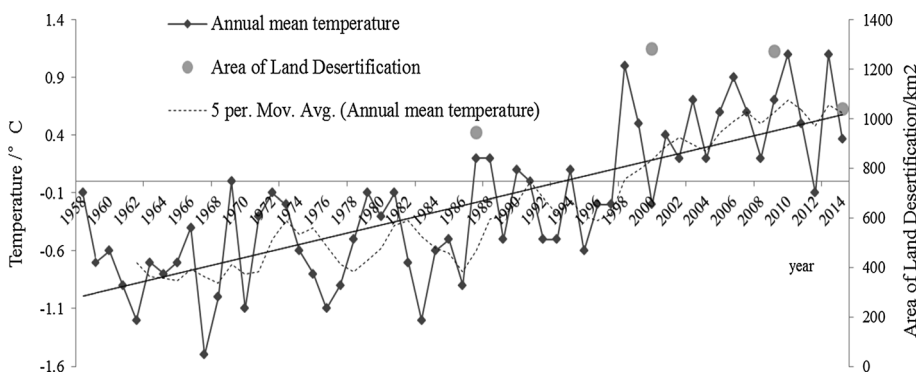

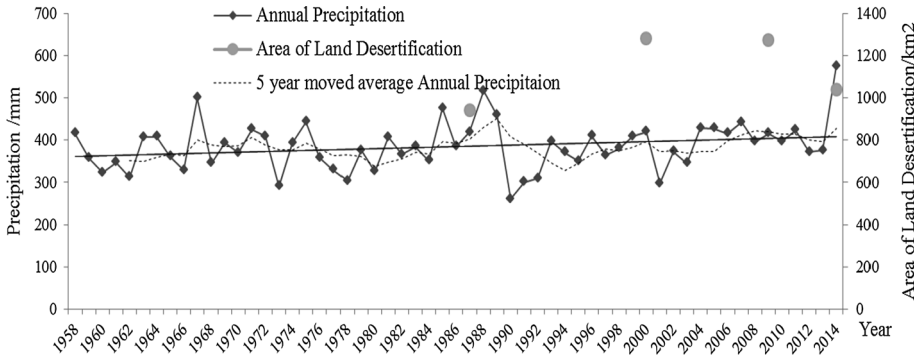Fig. 5 Changes of annual temperature from 1958 to 2014 in the Qinghai Lake watershed

Fig. 6 Changes of annual precipitation from 1958 to 2014 in the Qinghai Lake watershed

Moreover, storage and loss of moisture are extremely unbalanced, leading to a basin's drainage under overall water deficit (Fig. 7). Since the water deficit is negatively correlated with the degree of desertification, its negative value is taken to enable a comparison with desertification process. Hence, quite importantly prevention and control of the ADL can be quantified.

Specifically, large variations in annual mean temperature, precipitation and moisture deficit could be elicited from Figs. 5, 6, 7. The changes in meteorological conditions had a change trend corresponding to that of the aeolian desertification. Therefore, the dynamics of aeolian desertification can be attributed to the variations of climate conditions in different stages.

During the period of 1987–2000, the effects of precipitation accelerated the development of desertification during this period in the study area. In this stage, precipitation tended to drop gradually (Fig. 6). A 5-year moving average of moisture deficit in the river basin elicited to increase (Fig. 7). Consequently, desertification increased. On the other hand, the variation in annual mean precipitation was large, which easily led to frequent droughts. For example, annul mean precipitation is 384.68 mm; however, the highest precipitation was 515.8 mm in 1988, and the lowest was 260.1 mm in 1990 (Fig. 6). The difference was compatible with that in the lowest year. Similar trends could be found in
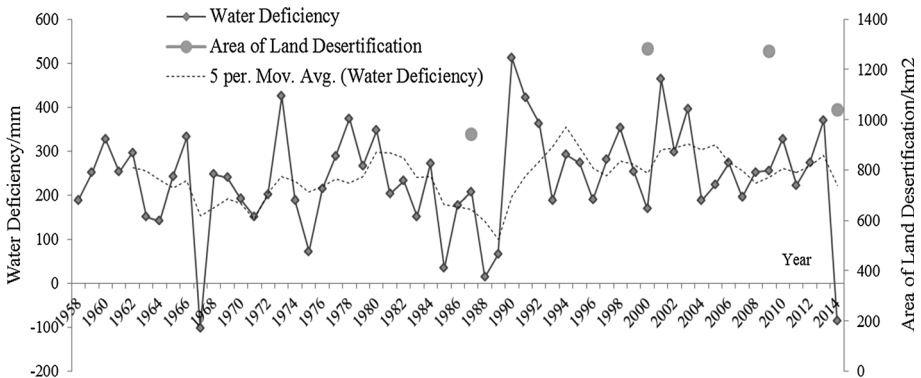

Fig. 7 Changes of annual water deficiency from 1958 to 2014 in the Qinghai Lake watershed

water deficiency as well (Fig. 7). From the period from 1987 to 2000, the precipitation decreased drastically, and the water deficiency increased rapidly, which should have contributed to the increased desertification during the study period.

After 2000, desertification in the study area showed a reverse trend. The annual precipitation and the basin moisture deficit remained relatively stable and even slightly decreased (Figs. 6, 7). A 5-year moving average of water deficit elicited a slowly decreasing water-deficit trend (Fig. 7). In particular, precipitation increased significantly during 2014 (Fig. 6). Hence, the development stages the land went through essentially were desertification stages from relatively stable to slightly decreasing. These phenomena took place over the periods from 2000 to 2009 and from 2009 to 2014. Besides, these phenomena could be attributed to reasonable human economic activity and desertification control measures as well.

Anthropogenic activities, which include over-reclaiming, overgrazing and excessive forest cutting, had an important impact as well on the process of desertification. Statistics show that population density had a significant increasing trend over the past 30 years in the QLB. Population density increased from 21,000 people in 1980 to 42,000 people in 2010 (Fig. 8), with an increase of 100 %. With rapid population growth, food requirement also increased. Farmland areas significantly increased after 1987; however, the farmland areas are stringently controlled since the year 2001 (Fig. 9), which is contributed to the national projects and measures that have been taken, such as abandoning and revegetating farmland on unsuitable land to produce forests or grassland.

Before the year 2000, particularly since 1980, with a fast growth of the population (Fig. 8), farmland area was especially needed (Fig. 9). Opposite interests developed between increasing demands in agricultural production and hosing from the population which had settled around the Lake. Natural resources degradation was prominent, and the phenomenon of grassland deterioration and cultivated land reclamation was a very hard problem popping up. This resulting in grassland degradation, soil erosion and an increase in land desertification worsened.

After 2000, a series of projects were implemented. The project of "Returning farmland to forest and grassland" and "The research and demonstration on the control technology of land desertification" were implemented. In particular, the project of the "Comprehensive treatment of the ecological environment of QLB" carried out by the Qinghai provincial government starting from May 2008 led to a series of prevention and control measures to harness land desertification, was launched. Population (Fig. 8) and farmland areas (Fig. 9)
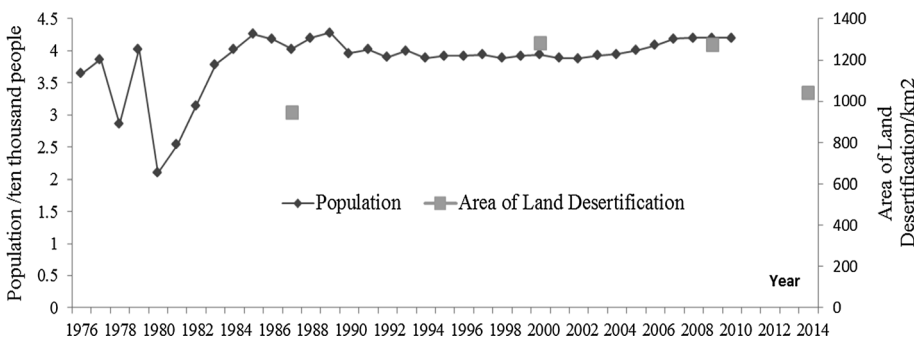

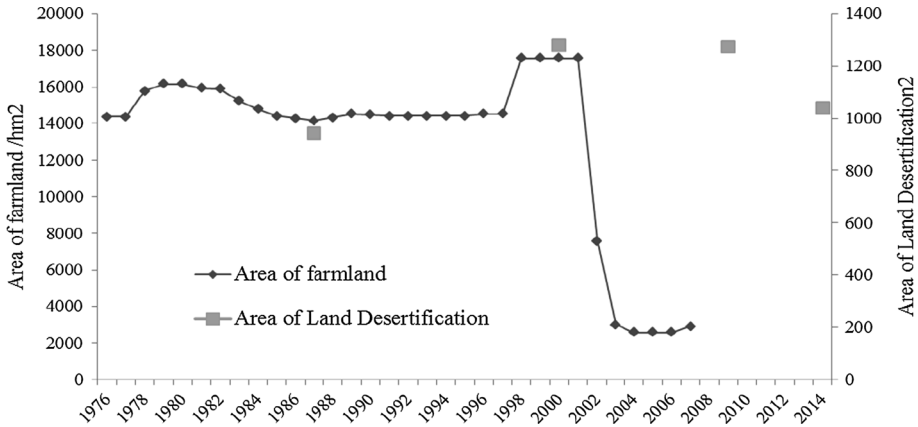Fig. 8 Population statistics of Gangcha County from 1976 to 2010 in the Qinghai Lake watershed

Fig. 9 Area of farmland in Gangcha County from 1976 to 2007 in the Qinghai Lake watershed

become under more stringent control. As a result, land desertification management in the region around Qinghai Lake has achieved some remarkable results during recent years. Actually, desertification has now started to gradually decrease.

6 Conclusions

Supported by RS and GIS technology, areas around Qinghai Lake were defined as study areas. The monitoring and analysis of the temporal and spatial variations of ADL by applying data of multi-source RS imagery, led to the following conclusions:

(1)   The surface area of land desertification in regions around Qinghai Lake is 1039.72 km^2 accounting for 6.51 % of total study area monitored in this region. The area of the extremely severe ADL is 469.78 km^2, accounting for 2.94 % of the study areas surface. Non-desertified land amounts to an area of 8207.71 km^2 and represents 51.37 % of the total study area. It is predominately covered with grassland.

(2)   The ADL of Qinghai Lake has increased from 942.99 km^2 in 1987 to 1039.72 km^2 in 2014. During this period, desertified area increased with a marginal 96.74 km^2. Over the recent 28 years, ADL in regions around Qinghai Lake has experienced a rapid expansion, followed by a relatively stable period followed by a gradual decline in desertification. Prior to 2000, land desertification in areas around Qinghai Lake expanded rapidly. Since the year 2000, ADL tended to stabilize and decrease.

(3)   The dynamics of desertification process changes around Qinghai Lake is the result of a combined effect of natural and anthropogenic factors. Before 2000, the water deficit in the river basin increased. Meanwhile, the pressure of an increasing human population led to an excessive land reclamation and overgrazing. This kicked off different types and degrees of desertification. After 2000, the water deficit in the river basin became smaller, at the same time, along with the start-up and implementation of projects cited earlier, desertification and vegetation recovery began to bear fruit, and the regional ecological environment started to achieve a more durable demographic, ecological and agricultural cycle.

References

Alatorre LC, Beguería S (2009) Identification of eroded areas using remote sensing in a badlands landscape on marls in the central Spanish Pyrenees. Catena 76:182–190

Ding Y, Liu F (1995) Effect of climatic change of water balance of Qinghai lake basin for recent thirty years and possible tendency. Scientia Geographica Sinica 2:128–135 **(In Chinese)**

Duan HC, Wang T, Xue X et al (2014) Dynamics of aeolian desertification and its driving forces in the Horqin Sandy Land, Northern China. Environ Monit Assess 186:6083–6096

Gao J, Liu YS (2010) Determination of land degradation causes in Tongyu County, Northeast China via land cover change detection. Int J Appl Earth Obs Geoinf 12:9–16

Guo L, Sha Z, Ma Y et al (2010) The past 20 years of land desertification landscape pattern analysis of spatial variation of Qinghai Lake area. China Popul Resour Environ S1:119–123 **(In Chinese)**

Hu M, Tian L, Zhang D, LI S, Gao S (2012) Study on dynamic changes of aeolian desertification lands around Qinghai Lake in recent 30 years based on remote sensing and GIS. J Desert Res 4:002 **(In Chinese)**

Hu G, Dong Z, Lu J, Yan C (2015) The developmental trend and influencing factors of aeolian desertification in the Zoige Basin, eastern Qinghai–Tibet Plateau. Aeolian Res. doi:10.1016/j.aeolia.2015.02.002

Jing Y, Zhou S, Wu F, Zhang Q (2011) Study on optimal bands selection of Sandy Land information extraction in Sandy Land monitoring based on land sat remote sensing data. Chin Agric Sci Bull 17:029 **(In Chinese)**

Le Houérou HN (1996) Climate change, drought and desertification. J Arid Environ 34:133–185

Liberti M, Simoniello T, Carone MT et al (2009) Mapping badland areas using LANDSAT TM/ETM satellite imagery and morphological data. Geomorphology 106:333–343

Liu JY, Liu ML, Zhuang DF et al (2003) Study on spatial pattern of land-use change in China during 1995–2000. Sci China (D) 46:373–384

Roberto JF (2002) Do humans create deserts? Trends Ecol Evol 17:6–7

Roy DP, Wulder MA, Loveland TR et al (2014) Landsat-8: science and product vision for terrestrial global change research. Remote Sens Environ 145:154–172

Shen W, Li H, Sun M, Jiang J (2012) Dynamics of aeolian sandy land in the Yarlung Zangbo River basin of Tibet, China from 1975–2008. Glob Planet Change 86:37–44

Shi YF, Shen YP, Li DL et al (2003) Discussion on the present climate change from warm-day to warm-wet in Northwest China. Quat Sci 23:152–164 **(In Chinese)**

Wang L, Ha S (2004) Advance in desertification research of Horqin Sandy Land. J Nat Disasters 13:8–14 **(In Chinese)**

Wang XM, Dong ZB, Yan P et al (2005) Wind energy environments and dune field activity in the Chinese deserts. Geomorphology 65:33–48

Wang T, Yan CZ, Song X, Xie J (2012) Monitoring recent trends in the area of aeolian desertified land using Landsat images in China's Xinjiang region. ISPRS J Photogramm Remote Sens 68:184–190

Wang T, Yan CZ, Song X et al (2013) Landsat images reveal trends in the aeolian desertification in a source area for sand and dust storms in China's Alashan Plateau (1975–2007). Land Degrad Dev 24:422–429

Yan CZ, Song X, Zhou YM et al (2009) Assessment of aeolian desertification trends from 1975's to 2005's in the watershed of the Longyangxia Reservoir in the upper reaches of China's Yellow River. Geomorphology 112:205–211

You Q, Kang S, Pepin N et al (2010) Climate warming and associated changes in atmospheric circulation in the eastern and central Tibetan Plateau from a homogenized dataset. Glob Planet Change 72:11–24

Yu W, Chen K (2002) Dynamic study on the remote sensing of desertified areas around the Qinghai Lake. J Salt Lake Res 10:48–51 **(In Chinese)**

Zhan X, Yan P (2012) Assessment and analysis of ecological benefit of combating desertification around Qinghai Lake. J Desert Res 32:1773–1778 **(In Chinese)**

Zhang H, Sha Z, Zhang T et al (2011) Spatial variation and driving force of sandy desertification in the peripheral area of the lake Qinghai in recent 20 years. J Arid Land Resour Environ 3:011 **(In Chinese)**

Zhao C, Lu R, Li J (2015) Land desertification and grain size characteristics of land surface deposits in the Qinghai lake watershed. J Desert Res 35:276–283 **(In Chinese)**